Reactive Behavior of the $[LiH_2]^+$ System I. Evaluation of the Lower-lying Electronic Potentials for the Collinear Geometries

E. Bodo,[†] F. A. Gianturco,*[,†] R. Martinazzo,[‡] and M. Raimondi[‡]

University of Rome "La Sapienza", Department of Chemistry, P.le A. Moro 5, 00185, Roma, and University of Milan, Department of Physical Chemistry and Electrochemistry and CNR center CSR SRC, V. Golgi 19, 20133, Milan

Received: June 19, 2001; In Final Form: October 12, 2001

The reactive behavior of the $[LiH_2]^+$ system is investigated by computing the potential energy surfaces (PES) for the collinear geometries. The three lowest-lying PESs have been obtained using a multireference valence bond approach and subsequently have been fitted with modified Laguerre functions. The results appear to exclude any significant nonadiabatic interaction between the first two electronic states and already suggest differences in the dynamical behavior of the title system when moving on each of these potential energy surfaces. Thus, at least within a collinear approach, a direct reactive dynamics should be expected for the ground-state reaction of $LiH^+ + H \rightarrow Li^+ + H_2$, while the formation of a temporary complex is suggested to occur for the partners interacting via the electronically excited PES pertaining to $LiH + H^+ \rightarrow Li + H_2^+$.

1. Introduction

In the modern studies of the early universe, it is usually accepted that chemistry began with the appearance of the first neutral molecule H_2, soon after the production of neutral atomic hydrogen through the radiative recombination of protons and electrons. Because of the absence of dust in the early universe, the chemistry that leads to the formation of the first molecules is driven by elementary reactions between atomic species.[1,2] As an example, lithium chemistry is thought to have been initiated by the formation of neutral Li through the radiative recombination of the Li^+ ion with electrons and to proceed with the formation of LiH species through the following radiative association processes,[3−6] the last one being the most efficient:[6]

$$\begin{aligned} Li + H &\rightarrow LiH + h\nu \\ Li^+ + H &\rightarrow LiH^+ + h\nu \\ Li^+ + H^- &\rightarrow LiH + h\nu \end{aligned} \qquad (1)$$

The LiH/LiH^+species, however, are being competitively depleted by the adiabatic processes

$$\begin{aligned} LiH + H^+ &\rightarrow Li + H^+_2 \\ LiH^+ + H &\rightarrow Li^+ + H_2 \\ LiH + H &\rightarrow Li + H_2 \end{aligned} \qquad (2)$$

We have explicitly avoided mentioning in the ionic network the reactions that would require a nonadiabatic transition between the two electronic states because we have already discussed them elsewhere and, from a preliminary study of their PES,[7,8] we found them likely to be forbidden. On the whole, the reactions $LiH^+ + H \rightarrow H^+_2 + Li$ and $LiH + H^+ \rightarrow H_2 + Li^+$, together with the charge exchange process ($LiH^+ + H \rightarrow LiH + H^+$), appeared to be quite improbable due to the absence of nonadiabatic interactions between the two electronic states.

The above list is already showing that ionic and neutral species involving atomic and molecular hydrogen and lithium are of importance in establishing the kinetic details of the lithium chemistry during the evolution of the early universe. It therefore follows that, to set up in some realistic way an evolutionary model, one must estimate the relative abundances of the chemical species by taking into account the chemical reactions listed above and many others that are connected to them and deemed to be relevant for the evolution of the primordial universe. We have already considered some aspects of this entangled network by looking at the neutral reaction in the simple collinear geometry[9] and at the behavior of its subreactive channels.[10]

Moreover, we have recently also sampled the subreactive configurational space of $LiH + H^+$ in order to estabilish the rovibrational heating efficiency of LiH by proton impact.[7] Since for this system the possible reactions[2] should be taken into account, we will first consider them here by looking at the collinear geometry of the partners' relative approach. In particular, great attention will be devoted to the Li−H−H geometry, which seems the most favorable one for the reactions[2] to occur, but we will also look at the other collinear arrangement, the H−Li−H situation. The evaluation of the full 3D reactive interaction potential is currently in progress in our laboratories for the first three electronic states and will be discussed elsewhere.[11] Meanwhile, we will show below that the analysis of the collinear situation is already capable of providing us with a lot of insight into the microscopic aspects of these reactions.

The work is presented in a sequence of two papers: in the present one we summarize in section 2 our knowledge of the energetics of the system, in section 3 we briefly describe the computational method used to obtain the potential energy surfaces, in section 4 we draw some general conclusions based on the topological properties of the PESs, and finally in sections 5 and 6 we describe the details of the interaction along with

* Corresponding author.
[†] University of Rome.
[‡] University of Milan.

10.1021/jp0123435 CCC: $20.00
Published on Web 11/16/2001

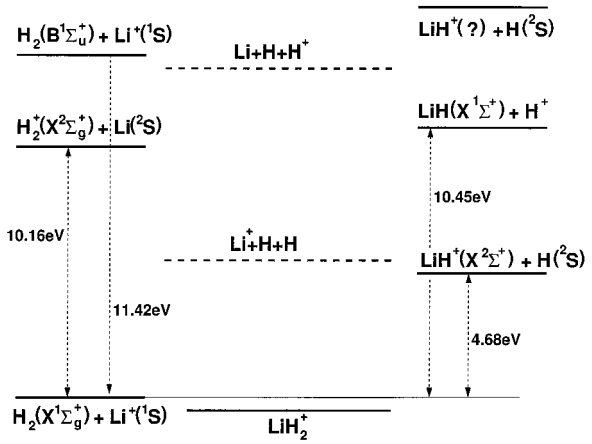

Figure 1. Energy correlation scheme for the LiH_2^+ complex. All values are in eV. In the middle of the diagram the triatomic dissociation thresholds (together with the ground bound state of the complex) are displayed. See text for further details.

the fitting procedure used to yield an analytical representation of the PESs.

2. The $[LiH_2]^+$ System

To understand the forces that drive the processes of eq 2, it is better to outline first the energetics of the system by looking both at partial (LiH+H and Li+H_2) and at the total (Li+H+H) break-up arrangements (see Figure 1). All the results reported there refer to adiabatic transitions, with the exception of the process involving the $H_2(X^1\Sigma) \rightarrow H_2(B^2\Sigma)$ transition where we have instead used the sudden difference.[12−14]

The neutral LiH molecule appears in the first excited state of the system because of the large difference between the ionization potential of the H atom (13.6 eV) and that of LiH molecule (7.9 eV for the vertical process) that leads to an asymptotic situation for the ground state in which the charge is localized on the LiH moiety. The LiH^+ molecule is a very weakly bound molecule, and therefore the ground-state break-up channel, Li^++H+H, is only slightly above the LiH^++H channel. On the other hand, the neutral H_2 molecule has an ionization potential greater than that of the Li atom, and therefore H_2 appears in the ground-state channel while the first excited electronic state dissociates on the left of the diagram as H_2^++Li.

The ground-state reactive surface therefore represents the interaction potential relevant for the study of the adiabatic processes

$$LiH^+ + H \rightarrow \begin{cases} Li^+ + H_2 \\ Li^+ + H + H \end{cases} \qquad (3)$$

In eq 3, the three body (3B) break-up channel has been considered because, as already mentioned, the very low binding energy of the LiH^+ molecule makes it already accessible at a collision energy of a few tenths of electronvolts. It is worth noting at this point that the colliding species in eq 3 have 1/4 probability of going through the PES of the singlet state, the other 3/4 being left for the $S = 1$ spin manifold. Since in the triplet state the parallel configuration of the two (hydrogenic) valence electrons prevents any reaction, for such spin manifold only the second process of eq 3 should be considered. In the following we will restrict our attention to the more interesting singlet state.

The first excited PES is relevant for the adiabatic reaction

$$LiH + H^+ \rightarrow Li + H_2^+ \qquad (4)$$

Since in this case the asymptotic partners experience strong electrostatic forces (due to the strong dipole of the LiH molecule and the substantial polarizability of the Li atom), the mentioned potential is characterized by the dipole-charge and charge-induced dipole interaction terms. Therefore, we will see two deep potential wells that have a marked influence on the dynamics and can support several triatomic bound states.

Possible nonadiabatic processes between the two states have been already discussed in previous works on this system.[8,7] In particular the main result of ref 8 was that the multisurface events could only be triggered by photon absorption or emission, which, however, would lead to rate constants that are too small to be relevant for the Li chemistry in the early universe environment. This important result follows from the large energy gap and from the difference in chemical properties between the two states. On one side, in fact, as we shall also see in the following, the asymptotic energy gap is not altered substantially in the interaction region, while on the other side the two electronic states retain a different nature: the positive charge, which is localized on the Li atom in the ground electronic state, is located on one (or two) of the H atoms in the excited state. This feature should make the nonadiabatic coupling elements too small to trigger a nonradiative transition.

On the contrary, possible nonadiabatic processes should be considered between the first and the second excited electronic states. Indeed, in the three-body break-up arrangement, both states dissociate as Li+H+H^+, which is doubly degenerate due to the presence of the charge. A previous analysis of the subreactive configurational space[7] revealed that deeply inside the interaction region the two excited states are somewhat interacting, because of a charge-exchange process that takes place between the two hydrogen atoms. The location and characterization of the possible conical intersection region in the full 3D space is an interesting subject in itself, but it is beyond the scope of this preliminary analysis, which considers instead the simpler 2D space of a collinear arrangement. Here we mention in passing another interesting aspect that arises in the asymptotic region of the LiH potential energy (as considered within the LiH_2^+ system) because of the degeneracy in the three-body break-up channel: a lower electronic state in which the charge appears exchanged over the two H atoms arises whenever one stretches the LiH bond in the presence of an isolated H^+. In Figure 2 we report (in the left panel) the relevant diatomic curves for the isolated LiH moiety and (right panel) the first lower lying curves obtained by stretching the LiH distance and keeping the HH distance fixed at a very large value (50 a_0 in the collinear LiHH configuration). The potential energy curve of the ground state of the right panel is simply the ground state of LiH^+ (white circles), which is being energy-shifted by the presence of a neutral hydrogen atom at infinite distance. The potential energy curve of the first excited state in the right panel can be easily thought of as arising from two diabatic curves, one which is that of the isolated LiH molecule (black squares) and the other is that of an electronically excited state of the isolated LiH^+ molecule (not shown in the figure, but very high in energy). This last state is the first excited state of the LiH^+ molecule and dissociates asymptotically as Li+H^+. Because of the presence of a shallow polarization well located at about 7.5 a_0,[13] this state, when considered in the presence of an isolated hydrogen atom, becomes lower in energy than that of the LiH (with an isolated H^+) and thus gives rise to a double minimum

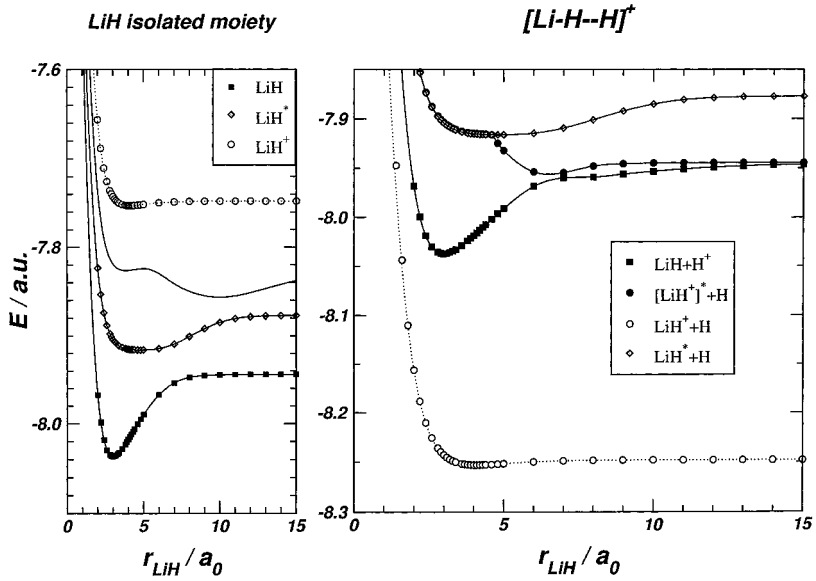

Figure 2. Potential energy curves as functions of the LiH distance. On the left the results for the first three electronic states of LiH and for the ground state of $LiH^+$are displayed. On the right the asymptotic situation of the LiH^+_2 complex when $r_{HH} \rightarrow \infty$ is shown. Total energies and lengths in au.

structure in the first excited asymptotic potential of the title system. At shorter range such an excited state becomes higher in energy than the state that correlates with the $A^1\Sigma^+$ state of LiH, and therefore the nature of second excited state depends strongly on the geometry at hand. This is the reason why in Figure 1 we left unspecified the labeling for that asymptotic situation. Since this asymptotic feature disappears in the interaction region (where the different electrostatic character of the two states is enhanced by the reduced distances), in the following we will neglect such effect. Indeed, our purpose is to obtain some information on the low energy processes occurring in the first excited states for which we could safely assume that an electronically adiabatic picture is sufficiently accurate.

3. The MRVB Calculation Scheme

The ab initio method that we have employed here is the multireference valence bond[15] approach within a spin coupled formulation.[16,17] Since this method has been described in detail elsewhere (in ref 15 technical details concernig our system are also reported), we will only give here a brief outline of it.

In the modern valence bond method, the nonorthogonal configuration interaction wave function is built starting with the spin-coupled (SC) wave function that acts as a single reference function. The SC wave function for N electrons can be written in the form

$$|\Psi_{SC}^{(SM)}\rangle = A[|\phi_1\rangle|\phi_2\rangle \cdots |\phi_N\rangle|SM\rangle] = A\,[|\Phi\rangle|SM\rangle] \quad (5)$$

where $|\phi_1\rangle$ represents a singly occupied non orthogonal orbital and $|SM\rangle$ is the total spin function, which is an eigenfunction of the $\mathbf{S}^2$and $\mathbf{S}_z$ operators with quantum numbers S and M. The total spin function is expanded as a combination of linearly independent N-electron spin eigenstates

$$|SM\rangle = \sum_{k=1}^{f_S^N} C_{Sk}|SM, k\rangle \quad (6)$$

where f_S^N is the dimension of the spin space. An ab initio SC calculation consists of the variational optimization of the coefficients C_{Sk}, which appear in eq 6, and of the orbitals, which appear in eq 5 expanded, as usual, onto a basis set. In general, this is carried out simultaneously without any constraint by minimizing the energy with respect to all of the parameters with an efficient modified Newton−Raphson algorithm.

The SC function correctly accounts for almost all nondynamical correlation and, in addition, turns out to be an excellent starting point for constructing very compact, multiconfigurational wave functions of the ground electronic state according to what we called the spin coupled valence bond (SCVB) model. In fact, a set of virtual orbitals can be added to each occupied orbital, either by a conventional diagonalization of effective monoelectronic operators[18] or by a perturbative multiconfigurational approach recently implemented.[19,20] In this last approach we associate to each of the N occupied orbitals $|\phi_i\rangle$ a virtual one, $|\phi_i^+\rangle$, and we construct a multiconfigurational wave function consisting of the SC configuration plus double excited configurations

$$|\Psi\rangle = c_0|\Psi\rangle + \sum_{i,j} c_{ij}|\Psi ij\rangle \quad (7)$$

where

$$|\Psi_{ij}\rangle = A[|\phi_1\rangle|\phi_2\rangle \ldots |\phi_i^+\rangle \ldots |\phi_N\rangle\,|SM\rangle] \quad (8)$$

The set of virtual orbitals $\{|\phi_i^+\rangle\}$ is then optimized by minimizing the second-order perturbative correction to the SC energy and used as "virtual space" into which vertical excitation of the occupied orbitals can take place.

This procedure can be extended to more than one reference function whenever a suitably spin coupled excited wave function can be obtained. We have recently shown how a large number of such functions can be obtained by imposing simple orthogonality constraints between the ground-state SC orbitals and the ones of the function that we are looking for. In particular, with a suitable choice of the active space and of the orthogonalization scheme, a very small number of reference functions is sufficient to achieve an overall high accuracy. We have already shown in ref 15 that an accurate wave function for the LiH_2^+ reactive configurational space can be obtained by means of two excited reference functions, one obtained from a 1:N orthogonalization

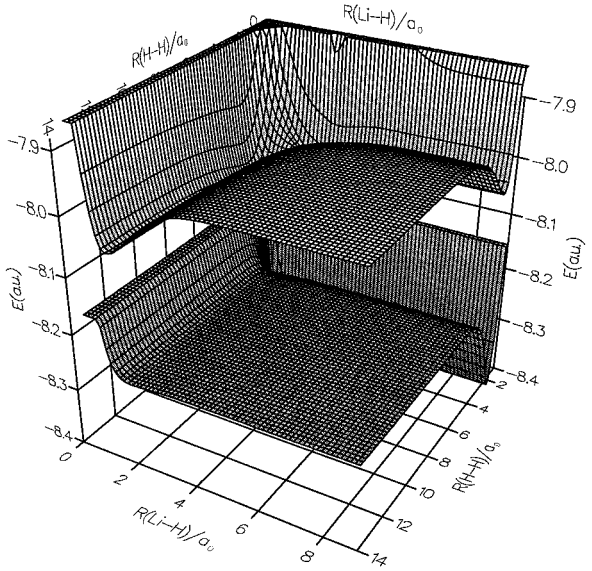

Figure 3. First and second roots in three dimensions as a function of r(Li−H) and r(H−H). The points are obtained from the analytical fitting of the ab initio values (see text).

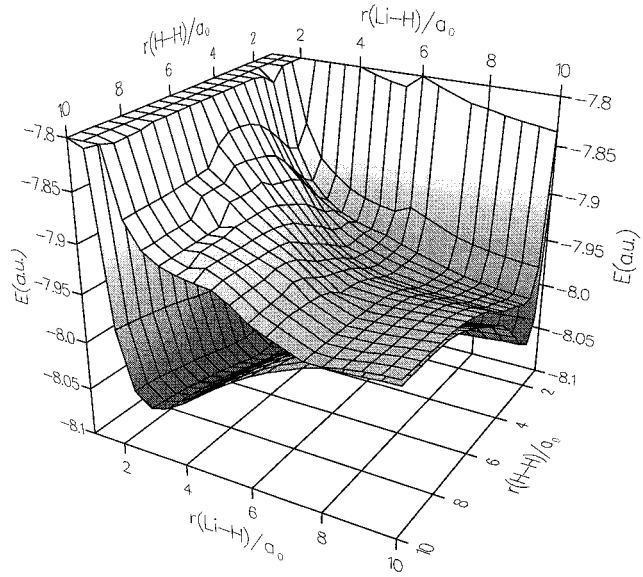

Figure 4. Second and third roots in three dimensions as a function of r(Li−H) and r(H−H). The points are the raw ab initio values (see text).

scheme and the other from a N:1 orthogonalization scheme. By using these reference functions, along with the ground-state one, we optimized a set of four pairs of virtual orbitals for each function and used this set for the full (vertical) excitation of the occupied orbitals into the virtual ones. In this way a multireference VB wave function was constructed with 321 configurations, corresponding to 617 structures when the spin degrees of freedom are taken into account. The basis set employed here consists of Li[10s4p2d/5s3p2d] and H[7s2p1d/5s2p1d]contracted Gaussian functions and has been already adopted in previous studies involving the LiH species.[9,20] We defer the interested reader to ref 15 for a more detailed discussion of the method. In the above work, some physical insight into the electronic features of the present system has also been gained by looking at the simple reference funtions. Moreover, a comparison between our results and FullCI data showed the high accuracy of our calculations.

4. General Properties of the Computed PESs

In the following we describe the calculated PESs of the two lowest electronic states in the two collinear geometries, along with the fitting procedure used to obtain an analytical representation of such potentials. The surfaces have been calculated on a rather dense grid of the two interatomic distances. For the Li−H−H geometry we have computed the potentials on a regular grid ranging from 1.0 a_0 to 11.0 a_0 for the LiH interatomic distance and from 0.5 a_0 to 10.0 a_0 for the HH distance. A single-point calculation has been performed every 0.5 a_0 throughout this ab initio region; the step size has been halved in a small region around the saddle point of the first excited state, that is, for 2.0 $a_0 \leq r_{LiH} \leq$ 5.0 a_0 and for 1.0 $a_0 \leq r_{HH} \leq$ 4.0 a_0. For the H_a−Li−H_b geometry we used an evenly spaced grid $r_{LiH_a} \geq r_{LiH_b} \in$ [1.0 a_0, 11.0 a_0] with a step size of 0.5 a_0.

An overview of the computed PESs is presented in Figures 3 and 4. In Figure 3 we give a 3D representation of the first two PESs for the Li−H−H geometry. We report the analytical fitting obtained from the first two PESs that shows the main features of the potentials: two electronic states that are well separated in energy and have a very different topology. Indeed, as we shall see better in the following, only the first excited state presents a nontrivial topology, having a saddle point between two deep wells in the asymptotic channels. In Figure 4 the first and second excited PESs (only ab initio points) are reported: although we are not interested in the highest state, we note that the two surfaces come into contact only in the asymptotic three-body break-up region and that the upper surface remains mainly repulsive. The third electronic state, in fact, correlates on one side with a mixed LiH*+H^+/LiH^+*+H state (see also Figure 2) and on the other side with an excited state of H_2^+ in the presence of a Li atom.

We can already anticipate, from the topological properties of the PES, some features of the dynamical behavior: while for the ground state the dynamics should be rather direct, for the excited state the dynamics is expected to be rather complex due to the likely presence of a large number of vibrational Feshbach resonances. Therefore, the processes on the ground-state surface should be occurring over rather short time intervals, while the dynamics confined to the first excited state could require a longer time to complete as a consequece of the probable formation of long-lived intermediates. Moreover, vibrational enhancement of the reactive outcome should be expected in the excited state as a consequence of the location of the saddle point of the surface, which corresponds to a streched geometry of the LiH molecule. All the above qualitative features will be further discussed below.

5. The PES of the Electronic Ground State

5.1. The Li−H−H Geometry. The ground-state potential energy function given by our calculations presents here a very simple structure, arising mainly from the two-body contributions. Indeed it is a relatively simple matter to fit the three-body (3B) nonadditive term, given by

$$V_{3B}(r_{LiH}, r_{HH}) = V(r_{LiH}, r_{HH}) - V_{LiH^+}(r_{LiH}) - V_{H_2}(r_{HH}) - V_{LiH^+}(r_{LiH} + r_{HH})$$

where the last term represents the potential acting between the lithium atom and the outer H atom. The diatomic potentials have been chosen according to the properties of the ground-state electronic wave functions. Since the charge is always located on the Li atom, the diatomic potentials corresponding

to the two LiH have been chosen to be that of LiH^+. The asymptotic potentials have been obtained from additional calculations at larger distances, one at $r_{LiH} = 15\ a_0$ for the H_2 curves and the other at $r_{HH} = 50\ a_0$ for the LiH curves.

The parameters of the H_2 potential turn out to be $D_e = 4.612$ eV and $r^e = 1.421\ a_0$; it supports 14 vibrational bound states, of which the lowest one has a dissociation energy of $D_0 = 4.348$ eV. These values compare favorably with those of refs 12, 21, 13, 22. For the LiH^+ potential we compute $D_e = 0.138$ eV, $r^e = 4.107\ a_0$, and 5 vibrational levels, the lowest lying yielding $D_0 = 0.111$ eV.

We fitted the 3B with the following functional form,

$$V_{3B}(r_1, r_2) = V_{SR}(r_1, r_2)\cdot(1 - f) + V_{LR}(r_1, r_2)\cdot f$$

where r_1 and r_2 now correspond to r_{LiH} and r_{HH}, respectively. Here V_{SR} is the short-range potential, f is a shape function of the form

$$f(r_1, r_2) = \frac{1}{1 + e^{r_1 - \rho_1}} \frac{1}{1 + e^{r_2 - \rho_2}}$$

(with ρ_1 and ρ_2 fixed respectively to 7.0 a_0 and 9.0 a_0) and V_{LR} is the long-range tail of the 3B potential,

$$V_{LR}(r_1, r_2) = -\frac{1}{2(r_1 + r_2/2)^4}(\alpha_{H_2}(r_2) - 2\alpha_H)$$

in which α_{H_2} is the polarizability curve of the hydrogen molecule and α_H is the polarizabilty of the hydrogen atom (4.50 in atomic units). For the first curve we used an analytic fitting of the data of ref 23, further corrected to ensure the right asymptotic behavior. The short-range potential, V_{SR} is the term that was actually fitted: we wrote it as

$$V^{SR}(r_1, r_2) = \sum_{n,m=0}^{4} b_{nm} L_n(r_1) L_m(r_2)\, e^{-\beta(r_1 + r_2)} \qquad (9)$$

(where L_n, L_m are Laguerre polynomials). We optimized the 50 parameters $\{b_{nm}\} \cup \{\beta_{nm}\}$, minimizing the square deviation by using the efficient Levenberg-Marquadt method.[24] Since for $\beta_{nm} = 0.5$ the basis functions reduce to products of ordinary Laguerre functions, we used the coefficients of a preliminary linear optimization as a guess for the nonlinear optimization. The resulting fitting was fairly good, having a standard deviation of 0.009 eV.

In Figure 5 we report a contour map of the fitted PES. As already mentioned, the surface is fairly uneventful and shows one deep and narrow channel corresponding to the H_2 molecule formation and a shallow and broad channel corresponding to LiH^+ formation.

5.2. The H−Li−H Geometry. In the other arrangement the 3B contribution is also fairly straightforward to obtain. There again we obtained its contribution to the total potential by subtracting the diatomic curves of the two possible molecular fragments (LiH^+, H_2). However, in this case a simple linear fitting with ordinary Laguerre functions was sufficient to achieve a very small standard deviation: 0.001 *eV*with 5*5 Laguerre functions. Note that the location of the charge on the Li atom makes the 3B long-range contribution to the potential vanish at large distance. A contour map of the fitted surface is reported in Figure 6.

6. The First Electronically Excited PES

6.1. The Li − H − H Arrangement. The first excited surface has a more complicated structure than the ground-state, mainly

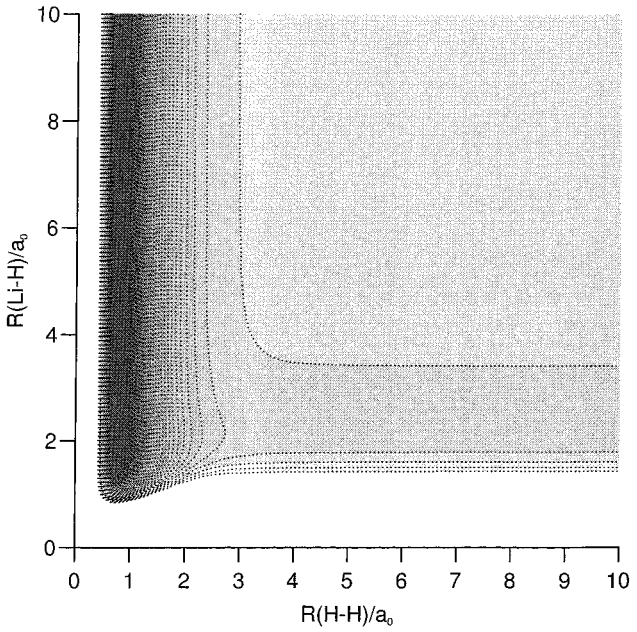

Figure 5. Contour plot of the ground-state PES for the Li−H−H geometry. Darker areas correspond to minima in the potential.

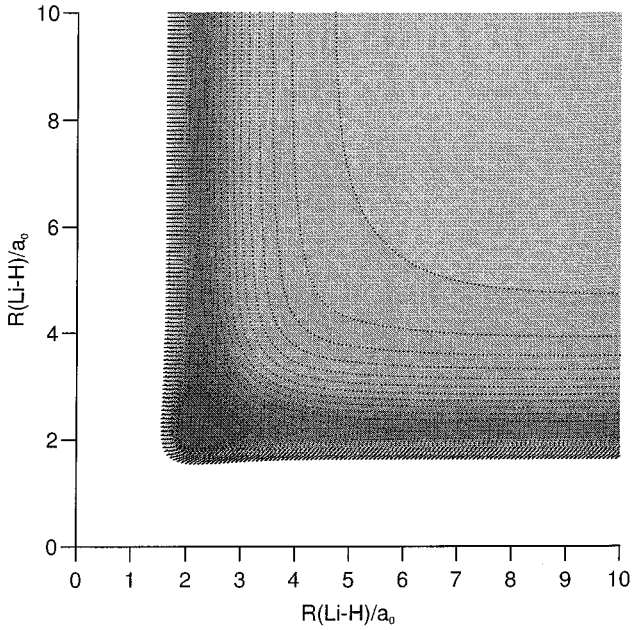

Figure 6. Contour plot of the ground-state PES for the H−Li−H geometry. Darker areas correspond to minima in the potential.

because of the different electrostatic forces that are now acting between the reagents and between the products. Here a 3B potential has been obtained by considering the charge located on one of the two *H* atoms:

$$V_{3B}(r_{LiH}, r_{HH}) = V(r_{LiH}, r_{HH}) - V_{LiH}(r_{LiH}) - V_{H_2^+}(r_{HH}) - V_{LiH^+}(r_{LiH} + r_{HH})$$

In this formula V_{LiH} is the LiH curve (the *diabatic* curve in Figure 2) and V_{LiH^+} is the diatomic curve of LiH^+ in its first electronic excited state, which dissociates as $Li+H^+$. Our LiH curve has $D_e = 2.466$ eV, $R = 2.977\ a_0$, and supports 25 vibrational states, the first one with a dissociation energy of $D_0 = 2.392$ eV (for a comparison of the molecular parameter see refs 12, 13, 22). The H^+_2 molecule turns out to have $D_e = 2.779$

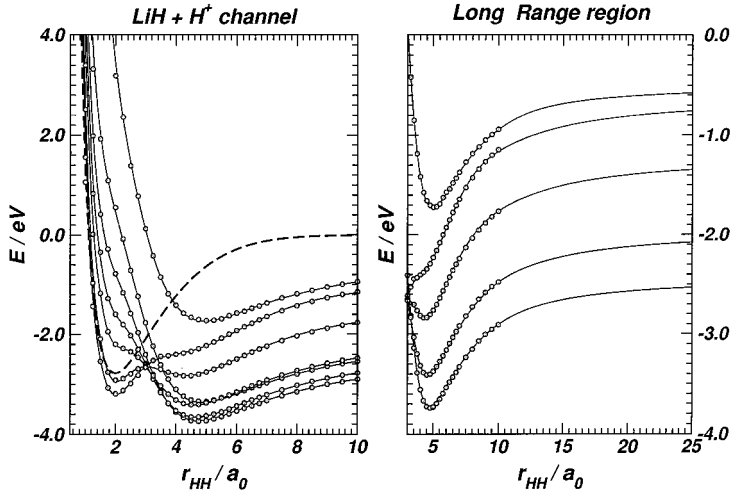

Figure 7. Left panel: potential energy curves for different r(LiH) values along the r(HH) coordinate. Solid lines are the analytical fitting functions, while the open circles show the raw ab initio points. The dashed line is the asymptotic H_2 potential. Right panel: long-range region joining the ab initio points and the fitting asymptotic function.

eV, $R = 1.998\ a_0$, and supports 18 vibrational states, the first one with $D_0 = 2.637$ eV. Since in this case the 3B term has very important contributions coming from the long-range tails of the interaction, we wrote it in the form

$$V_{3B}(r_1, r_2) = V_{SR}(r_1, r_2)f_1f_2 + V^{(1)}_{LR}(r_1, r_2)(1 - f_1) + V^{(2)}_{LR}(r_1, r_2)(1 - f_2)$$

where

$$f_1 = \frac{1}{1 + e^{0.5(r_1+r_2)-\xi_2}} \quad f_2 = \frac{1}{1+e^{r_1-\xi_1}}$$

and

$$V^{(1)}_{LR}(r_1, r_2) = -\frac{\mu(r_1)}{(0.5\cdot r_1 + r_2)^2}$$

is the dipole potential term obtained from the data of ref 23 and $V^{(2)}_{LR}$ is the analogous polarizability contribution (we used $\alpha_{Li} = 176.0$ au as obtaneid from our asymptotic potentials). The shape function f_1 switches on the dipole contribution when $0.5r_{LiH} + r_{HH} \geq \xi_1$, while f_2 switches on the polarization term only at large Li−H distances (for the dipole term it should be noted that the behavior of the dipole curve as a function of r(LiH) ensures that the contribution vanishes for large Li−H distances). The variables ξ_1 and ξ_2, and those entering in the expansion of the short-range contribution, have been subjected to the same optimization procedure used for the ground-state PES, the only difference being that the short-range term has been written as

$$V_{SR}(r_1, r_2) = V_0 + \sum_{n,m=0}^{5} b_{nm}L_n(\rho^{(1)}_n)L_m(\rho^{(2)}_m)\, e^{-0.5(\rho^{(1)}_n + \rho^{(2)}_m)} \tag{10}$$

where

$$\rho^{(1)}_n = \beta_n\left(\frac{r_1}{r_{LiH,e}} - 0.5\right) \text{ and } \rho^{(2)}_n = \beta_n\left(\frac{r_2}{r_{H_2^+,e}} - 0.5\right)$$

($r_{M,e}$ terms being the equilibrium distances of the diatomic molecules). In this case the origin of the coordinates of the Laguerre functions has been slightly shifted to better model the interaction region. It turned out that the final fitting function had to be slighlty modified in the (extrapolated) short-range region (i.e., $\rho^{(i)} \ll 0$) to avoid anomalous behavior of the analitycal PES.

We optimized a total of 51 parameters using the data points with energy of less than 1.0 eV (with the zero of the potential put in the triatomic dissociation limit). The resulting fit turned out to have a standard deviation of 0.018 eV. Figures 7 and 8 show a comparison between the fitted PES and the original ab initio data, both for the entrance channel and for the exit channel of the reaction.[4] In the right panels we report an enlarged view of the regions to show how smoothly the long-range term has been added to the potential of the ab initio region. Finally, in Figure 9 we report a contour plot for the fitted surface of the upper electronic state. It presents an interesting topology caused mainly by the strong electrostatic forces that are now acting at large and intermediate distances between the fragments. As is evident from the figure, the surface presents two well localized minima and a saddle point. The minimum in the reactants region (along r_{HH}) is at an energy of ~ -1.26 eV with respect to the LiH+H^+ arrangement and of ~ -3.74 eV with respect to the dissociation limit (Li+H+H^+); the other is ~ -0.46 eV in reference to H_2^++Li and ~ -3.24 eV to the dissociation limit. The "barrier" is located at -2.655 eV with respect to the dissociation limit. The two LiH and H_2^+ asymptotes are respectively -2.47 eV and -2.78 eV in reference to the dissociative threshold and therefore the barrier is 0.185 eV *lower* in energy than the LiH+H^+ asymptote and 0.125 eV *higher* than the Li+H_2^+ one. This is clearly illustrated by the minimum energy path on this surface, reported schematically in Figure 10. One should note, however, that the position of the "left" asymptote is different from what is shown in the figure since the cut of it is taken in a region where the dipole charge contribution is still not negligible, and thus it lowers the *real* asymptote of about 0.13 eV. It is interesting to note that the transition state involves a geometry in which the LiH and the HH bonds are markedly "stretched" ($r_{LiH} \sim 5.0\ a_0$ and $r_{HH} \sim 3.0\ a_0$), and thus one should expect enhancing of the reaction probability when vibrationally excited LiH (or H_2^+ for the reverse reaction) is involved, while one should find a more limited reaction efficiency when starting with LiH (H_2^+) in their vibrational ground state. Apart from these simple considerations,

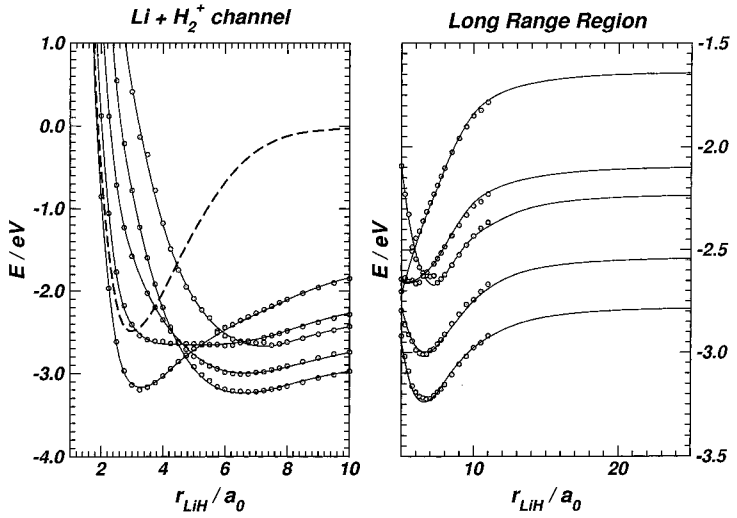

Figure 8. Left panel: potential energy curves for different r(HH) values along the r(LiH) coordinate. Solid lines are the analytic fitting functions, open circles are the raw ab initio points, and the dashed line is the asymptotic LiH potential curve. Right panel: long-range region joining the ab initio points and the fitting asymptotic function.

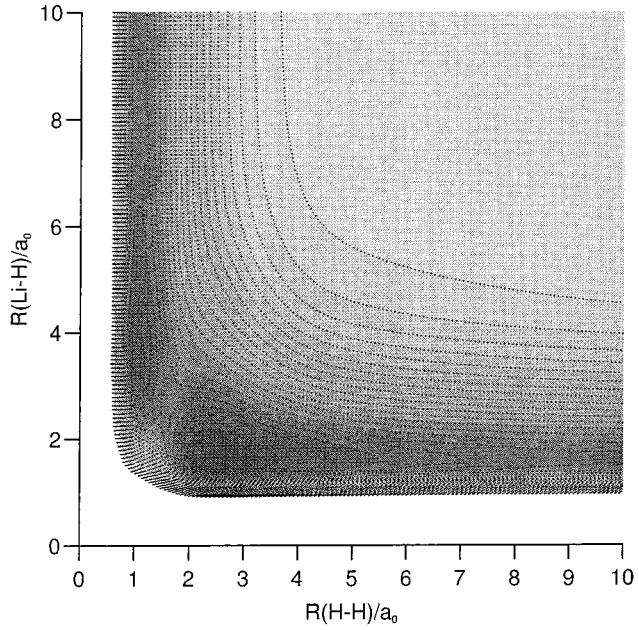

Figure 9. Contours for the first electronic state in the Li−H−H geometry. Darker areas correspond to minima on the potential energy surface.

however, the topology of the surface is such that only a direct treatment of the dynamics could give us more quantitative details.

6.2. The H−Li−H Arrangement. The collinear H−Li−H arrangement does not play a significant role for the reaction,[4] and therefore our computed raw points have not been further fitted with an analytical function. Its shape originates mostly from the repulsive dipole-charge contribution and from the symmetry of the system, where the repulsive interaction gives rise to an activation barrier between the two symmetry-related channels. In contrast to this situation, it should be noted that the ground-state counterpart could instead acquire some importance when studying the collision-induced dissociation processes.

7. Present Conclusions

In this work we have reported our new results from an ab initio calculation for the collinear reactive configurational space

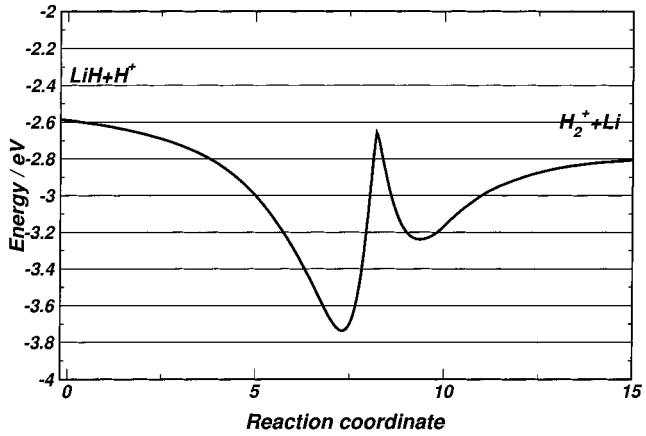

Figure 10. Minimum energy path for the first electronically excited state of the title system.

in the LiH_2^+ system. Although the potential energy surfaces are only preliminary to the study of the full dimensional evaluation of the interaction, we can already draw some interesting conclusions about the dynamics that is likely to take place in this system. We have recently shown[8] that in the early universe environment only adiabatic processes should be taken into account in reactions involving the first two electronic states of the title system. Therefore, in the present, more specific analysis of interaction energetics we have proceeded to obtain an analytical representation of the most interesting two-dimensional potentials in order to acquire a more quantitative description of them, which would then allow us to carry out collinear scattering studies. For the ground-state processes, owing to the possible occurrence of three-atom break-up events, the collinear model appears to be already of some significance and we will therefore present in the following paper (paper II) the collinear treatment of the reaction. The corresponding study of the dynamics occurring on the excited state PES, although of importance because of the very long range of action of the potential, is of relevance chiefly for an accurate evaluation of the subreactive rovibrational energy transfer dynamics in $LiH+H^+$. We have already computed the corresponding three-dimensional potential points relevant for this scattering system[7] and therefore the collinear reactive calculations that we have also planned for it can give us further information on the importance of the reactive processes in the most favorable

arrangement. These results will be presented elsewhere in conjunction with the analysis of the inelastic rovibrational scattering calculations.[25]

A Fortran77 function routine which furnishes the analytical representation of the PESs here described could be provided on request to the authors. The parameter values are not given here for reasons of brevity.

References and Notes

(1) Lepp, S.; Shull, J. M. *Astrophys. J.* **1984**, *280*, 465.
(2) Lepp, S.; Stancil, P. C. in *The Molecular Astrophysics of Star and Galaxies*; Hartquist, T. W., Williams, D. A., Eds.; Clarendon Press: Oxford, 1998.
(3) Dalgarno, A.; Stancil, P. C.; Kirby, K. *Astrophys. J.* **1996**, *458*, 397.
(4) Gianturco, F. A.; Giorgi, P. G. *Phys. Rev. A* **1996**, *54*, 4073.
(5) Gianturco, F. A.; Giorgi, P. G. *Astrophys. J.* **1997**, *479*, 560.
(6) Dickinson, A. S.; Gadea, F. X. *Mon. Not. R. Astron. Soc.* **2000**, *318*, 1227.
(7) Bodo, E.; Gianturco, F. A.; Martinazzo, R.; Forni, A.; Famulari, A.; Raimondi, M. *J. Phys. Chem. A* **2000**, *104*, 11972.
(8) Bodo, E.; Gianturco, F. A.; Martinazzo, R.; Raimondi, M., in press.
(9) Clarke, N. J.; Sironi, M.; Raimondi, M.; Kumar, S.; Gianturco, F. A.; Buonomo, E.; Cooper, D. L. *Chem. Phys.* **1998**, *233*, 9.
(10) Bodo, E.; Gianturco, F. A.; Martinazzo, R.; Raimondi, M. *Eur. Phys. J. D* **2001**, *15*, 321.
(11) Bodo, E.; Gianturco, F. A.; Martinazzo, R.; Raimondi, M. in preparation.
(12) Huber, K. P.; Herzberg, G. *Molecular spectra and molecular structure*; Van Nostrand Reinhold: New York, 1979.
(13) Stwalley, W. C.; Zemke, W. T. *J. Phys. Chem. Ref. Data* **1993**, *22*, 87.
(14) Moore, C. E. *Atomic Energy Levels*; National Bureau Standards, Cir. No. 467; GPO: Washington, DC, 1971.
(15) Martinazzo, R.; Famulari, A.; Raimondi, M.; Bodo, E.; Gianturco, F. A. *J. Chem. Phys.* **2001**, *115*, 2917.
(16) Cooper, D. L.; Gerrat, J.; Raimondi, M. *Adv. Chem. Phys.* **1987**, *69*, 319.
(17) Cooper, D. L.; Gerrat, J.; Raimondi, M. *Chem. Rev.* **1991**, *91*, 929.
(18) Gerratt, J.; Raimondi, M. *Proc. R. Soc. London* **1980**, *A371*, 525.
(19) Clarke, N. J.; Raimondi, M.; Sironi, M.; Cooper, D. *Theor. Chem. Acta* **1998**, *95*, 1328.
(20) Gianturco, F. A.; Kumar, S.; Pathak, S. K.; Raimondi, M.; Sironi, M.; Gerrat, J.; Cooper, D. L. *Chem. Phys.* **1997**, *215*, 227.
(21) Eyler, E. E.; Melikeki, N. *Phys. Rev. A* **1993**, *48*, R18.
(22) Lee, H. S.; Lee, Y. S.; Jeung, G. *J. Phys. Chem. A* **1999**, *103*, 11080.
(23) Hyamas, P. A.; Gerratt, J.; Cooper, D. L.; Raimondi, M. *J. Chem. Phys.* **1994**, *100*, 4417.
(24) Press, W. H.; Flannery, B. P.; Teukolsky, S. A.; Vetterling, W. T. *Numerical Recipes*; Cambridge University Press: Cambridge, 1986.
(25) Bodo, E.; Gianturco, F. A.; Martinazzo, R. *J. Phys. Chem. A* **2001**, *105*, 10994.